Reconfigurable microwave photonic filter based on parallel-cascaded microrings assisted with a Mach–Zehnder interferometer

2012 J. Opt. 14 065502

(http://iopscience.iop.org/2040-8986/14/6/065502)

IOP PUBLISHING JOURNAL OF OPTICS
J. Opt. **14** (2012) 065502 (5pp) doi:10.1088/2040-8978/14/6/065502

Reconfigurable microwave photonic filter based on parallel-cascaded microrings assisted with a Mach–Zehnder interferometer

Dengke Zhang, Xue Feng and Yidong Huang

State Key Laboratory of Integrated Optoelectronics, Department of Electronic Engineering, Tsinghua University, Beijing 100084, People's Republic of China

E-mail: x-feng@tsinghua.edu.cn

Received 14 March 2012, accepted for publication 2 May 2012
Published 30 May 2012
Online at stacks.iop.org/JOpt/14/065502

Abstract
A reconfigurable microwave photonic filter based on parallel-cascaded silicon microrings is proposed and demonstrated with numerical simulation. A Mach–Zehnder interferometer (MZI) is introduced between two adjacent microrings. Through tuning the MZI, the feedback ratios of adjacent rings can be tuned so that both the bandwidth and shape of filter response can be adjusted while the central wavelength remains constant and the sidelobes can also be remarkably suppressed.

Keywords: microwave photonic filters, parallel-cascaded microrings, Mach–Zehnder interferometer, reconfigurable

(Some figures may appear in colour only in the online journal)

1. Introduction

Microwavephotonic filters (MPFs) could process microwave signals in the optical domain with attractive characteristics, such as low loss, wide bandwidth, immunity to electromagnetic interference, as well as high operating frequency. It has been proposed that MPFs can be applied in the fields ranging from radar, satellite to wireless communications [1]. For such applications, reconfigurable MPFs are desired. As demonstrated, most reconfigurable MPFs are implemented with discrete photonic devices such as WDM couplers, $LiNbO_3$ modulators, fibers coils or fiber gratings as phase delay elements and an array of tunable lasers [2] or a spectrum-sliced broadband source as light source [3]. With such implementation, the footprint is rather large and the filter response is hard to control or tune.

Recently, a new kind of MPFs based on microrings (MRs) has attracted more and more attention. They are fabricated on a silicon-on-insulator (SOI) substrate and can be integrated with other optoelectronic components [4]. Pile *et al* investigated the operation principle of MR–MPF in theory, and the noise and distortion performance were analyzed as well [5]. Rasras *et al* demonstrated a notch MR–MPF with a size of 5×0.35 mm^2 for an optical processor [6], and Palaci *et al* realized a band-pass MPF based on a single MR with a size of 50×50 μm^2 for the optical processor [7]. In our previous work [8], the application of MR–MPFs on 60 GHz millimeter wave wireless personal area networks (WPAN) was investigated with numerical simulation.

Parallel-cascaded silicon MRs serving as optical filters have been widely studied because of unique characteristics including simple design and sharp edges [9, 10]. Generally, the parallel-cascaded microrings are simultaneously coupled to the input and output bus waveguide but are not coupled to themselves. Because the feedbacks of adjacent rings are like Fabry–Perot resonators, the response of filters relies on the feedback ratios. To synthesize the rational response of filters, apodization of the feedback ratios was proposed to suppress the sidelobes, and there are several algorithms to obtain optimum spectrum shapes [11]. However, the feedback ratios

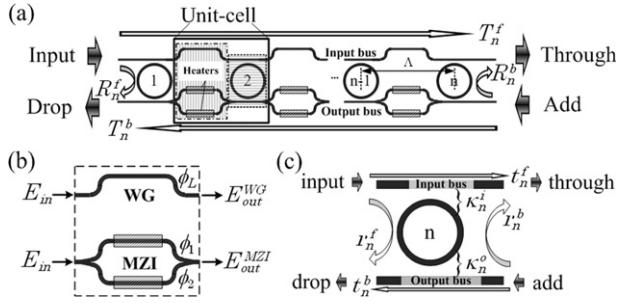

Figure 1. (a) Schematic setup of the filter based on MZI assisted parallel-cascaded MRs. (b) Comparison between MZI and an ordinary waveguide. (c) An arbitrary ring in (a).

are hard to tune after the device has been fabricated. In [12], a method of varying the coupling coefficients was proposed to tune the feedback ratios. But the resonance wavelength of microrings would also be changed with variation of coupling coefficients and the spectrum shape would consequently be distorted. In order to solve such a problem, we propose a new method to tune the feedback ratios with constant resonance wavelength.

In this paper, the reconfigurable MPF is based on Mach–Zehnder interferometer (MZI) assisted parallel-cascaded silicon MRs. The MZI is introduced between MRs so that the feedback ratio of adjacent rings could be tuned independently by controlling the phase shifters of MZI. As a result, a reconfigurable MPF with constant central wavelength can be achieved.

2. Structure and principle

Figure 1(a) shows the schematic setup of the proposed parallel-cascaded MRs assisted by MZI. As marked in the solid line box, a unit-cell of such a cascaded structure contains an MR with two buses, a Mach–Zehnder interferometer, and two heaters (or p–n junctions) on each arm serving as tuning elements. In contrast to general parallel-cascaded MRs, a MZI is introduced to tune the feedback ratio at the output bus in each unit-cell. For more clarity, the unit-cell is divided into two parts marked by boxes using dotted lines in figure 1(a). The enlarged figures of two such parts are depicted in figures 1(b) and (c), respectively.

Figure 1(b) shows an ordinary waveguide (marked as WG) and an MZI with heaters (or p–n junctions) on each arm to serve as a phase shifter. The length of the ordinary WG and the two arms of MZI are identical, so the phase delays from the 'input' port to the 'output' port of ordinary WG and MZI are equal without tuning, where such a normal phase delay is denoted as ϕ_{L}, and the output amplitude of ordinary WG ($E_{\mathrm{out}}^{\mathrm{WG}}$) and the MZI ($E_{\mathrm{out}}^{\mathrm{MZI}}$) are the same as $E_{\mathrm{in}}\mathrm{e}^{\mathrm{j}\phi_{\mathrm{L}}}$ with input amplitude E_{in}. Here, the phase delay of the upper (lower) arm ($\phi_{1(2)}$) with a phase shift ($\Delta\phi_{1(2)}$) due to thermal tuning is defined by $\phi_{1(2)} = \phi_{\mathrm{L}} + \Delta\phi_{1(2)}$. Then, the output of MZI is given by $E_{\mathrm{out}}^{\mathrm{MZI}} = (E_{\mathrm{in}}\mathrm{e}^{\mathrm{j}(\phi_{\mathrm{L}}+\Delta\phi_1)} + E_{\mathrm{in}}\mathrm{e}^{\mathrm{j}(\phi_{\mathrm{L}}+\Delta\phi_2)})/2$. Moreover, the output amplitude of MZI can be written as

$$E_{\mathrm{out}}^{\mathrm{MZI}} = E_{\mathrm{in}}\mathrm{e}^{\mathrm{j}\phi_{\mathrm{L}}}\left(\frac{\mathrm{e}^{\mathrm{j}\Delta\phi_1} + \mathrm{e}^{\mathrm{j}\Delta\phi_2}}{2}\right) = E_{\mathrm{in}}\mathrm{e}^{\mathrm{j}\phi_{\mathrm{L}}}A_{\mathrm{add}}\mathrm{e}^{\mathrm{j}\Delta\phi_{\mathrm{add}}} \quad (1)$$

where A_{add} and $\Delta\phi_{\mathrm{add}}$ are additional amplitude and phase shift, respectively. Equation (1) shows that a complex amplitude $A_{\mathrm{add}}\mathrm{e}^{\mathrm{j}\Delta\phi_{\mathrm{add}}}$ is added on the output amplitude of MZI after thermal (or electrical) tuning. Meanwhile the term $A_{\mathrm{add}}\mathrm{e}^{\mathrm{j}\Delta\phi_{\mathrm{add}}}$ is directly related to $\Delta\phi_{1,2}$ as shown in equation (1), so that an arbitrary value can be obtained by proper setting of $\Delta\phi_{1,2}$. Figure 2 shows the relationships between normalized $A_{\mathrm{add}}\mathrm{e}^{\mathrm{j}\Delta\phi_{\mathrm{add}}}$ and $\Delta\phi_{1,2}$. Because of such additional complex amplitude, the feedback ratios can be tuned and the filter response can be reconfigured in succession.

In figure 1(a), the terms of R_n^{f} or T_n^{f} represents the net forward reflection or transmission coefficient (defined as the amplitude ratio between the 'drop' or 'through' port and the 'input' port) for all n rings and the terms R_n^{b} or T_n^{b} represent the net backward reflection or transmission coefficient (defined as the amplitude ratio between the 'through' port or 'drop' and 'add' port) for all n rings. Figure 1(c) depicts the nth ring in the device of figure 1(a) and the terms of r_n^{f} and t_n^{f} are reflection and transmission responses of the nth ring compared

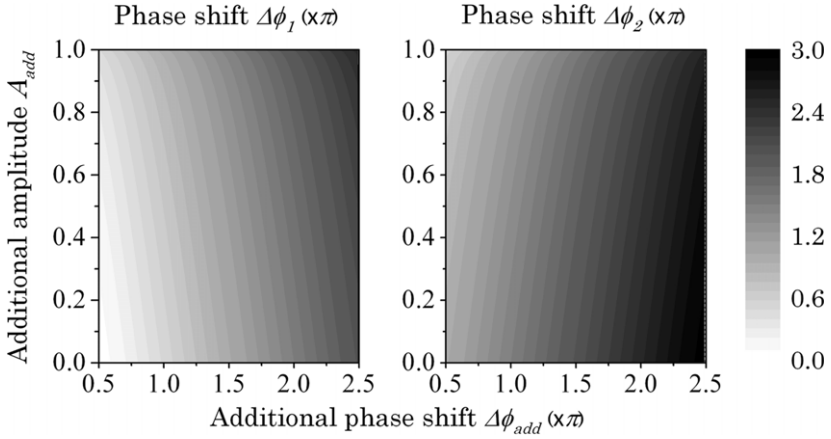

Figure 2. Relationships between $A_{\mathrm{add}}\mathrm{e}^{\mathrm{j}\Delta\phi_{\mathrm{add}}}$ and $\Delta\phi_{1,2}$.

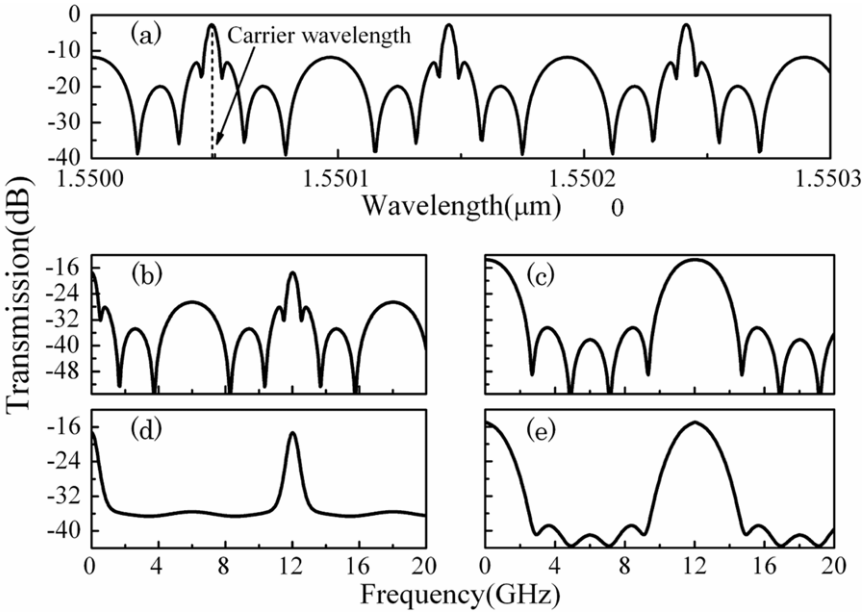

Figure 3. (a) Optical response of the device in figure 1(a). (b) The microwave response corresponds to (a). (c) The microwave response with appended phase tuning; (d) and (e) microwave responses with appended amplitude tuning based on (b) and (c), respectively.

to the 'input' port and the terms of r_n^{b} and t_n^{b} are related to 'add' port importation, respectively. The terms of $\xi_n^{i(o)}$ or $\kappa_n^{i(o)}$ represent self- or cross-amplitude coupling coefficients between the ring and input (output) bus. The overall reflection response $R_{\mathrm{N}}^{\mathrm{f}}$ of the full proposed structure with N rings can be deduced with recursive formulae

$$R_n^{\mathrm{f}} = R_{n-1}^{\mathrm{f}} + \frac{T_{n-1}^{\mathrm{f}} r_n^{\mathrm{f}} T_{n-1}^{\mathrm{b}} \mathrm{e}^{\mathrm{j}(\beta+j\alpha)2\Lambda} A_{\mathrm{add}} \mathrm{e}^{\mathrm{j}\Delta\phi_{\mathrm{add}}}}{1 - r_n^{\mathrm{f}} R_{n-1}^{\mathrm{b}} \mathrm{e}^{\mathrm{j}(\beta+\mathrm{j}\alpha)2\Lambda} A_{\mathrm{add}} \mathrm{e}^{\mathrm{j}\Delta\phi_{\mathrm{add}}}} \quad (2a)$$

$$T_n^{\mathrm{f}} = \frac{T_{n-1}^{\mathrm{f}} t_n^{\mathrm{f}} \mathrm{e}^{\mathrm{j}(\beta+\mathrm{j}\alpha)\Lambda}}{1 - r_n^{\mathrm{f}} R_{n-1}^{\mathrm{b}} \mathrm{e}^{\mathrm{j}(\beta+\mathrm{j}\alpha)2\Lambda} A_{\mathrm{add}} \mathrm{e}^{\mathrm{j}\Delta\phi_{\mathrm{add}}}} \quad (2b)$$

$$r_n^{\mathrm{f,b}} = \frac{\kappa_n^i \kappa_n^o \mathrm{e}^{\mathrm{j}(\beta+\mathrm{j}\alpha)\pi R}}{1 - \xi_n^i \xi_n^o \mathrm{e}^{\mathrm{j}(\beta+\mathrm{j}\alpha)2\pi R}} \quad (2c)$$

$$t_n^{\mathrm{f,b}} = \xi_n^{i,o} + \frac{\kappa_n^{i,o} \kappa_n^{i,o} \xi_n^{o,i} \mathrm{e}^{\mathrm{j}(\beta+\mathrm{j}\alpha)2\pi R}}{1 - \xi_n^i \xi_n^o \mathrm{e}^{\mathrm{j}(\beta+\mathrm{j}\alpha)2\pi R}} \quad (2d)$$

where β and α are the propagation constant and attenuation coefficient of the light wave mode, which are assumed to have a constant value both in waveguides and rings. R is the ring radius and Λ is the spacing between the adjacent rings. To keep the output amplitudes of all rings in phase, the spacing should satisfy the relation of $\Lambda = (m + 0.5)\pi/\beta (m \geq 1)$ [9]. R_n^{b} and T_n^{b} can be deduced with the same method as R_n^{f} and T_n^{f}.

In the front part of this section, the filter responses in the optical domain are obtained. Then after concerning the modulation format, the filter responses in the microwave domain could be obtained. Here, double-sideband plus carrier (DSB + C) modulation and symmetry carrier placement are assumed and the optical response $R_{\mathrm{N}}^{\mathrm{f}}$ is adopted for a band-pass filter. By applying the formula in [5], the microwave response of our proposed MPF could be obtained

$$H_{\mathrm{M}}(\omega_{\mathrm{m}}) \approx \frac{\mathrm{j}2\Re P_{\mathrm{c}}}{v_{\mathrm{m}}} J_0(m) J_1(m) R_{\mathrm{N}}^{\mathrm{f}}(\omega_{\mathrm{c}}) R_{\mathrm{N}}^{\mathrm{f}}(\omega_{\mathrm{c}} + \omega_{\mathrm{m}}) \quad (3)$$

where ω_{c} and ω_{m} are optical carrier and microwave signal frequency, respectively, v_{m} is the amplitude of the microwave signal, m is the modulation depth, $\Re$ is the responsivity of an ideal photodetector, P_{c} is the input laser power, and $J_n(\cdot)$ is the nth-order Bessel function of the first kind.

3. Simulation results

In the simulation, the MPF is considered as a five stage-cascaded structure and is assumed to be fabricated on an SOI substrate with a shallow-ridge waveguide. The dimensions of the waveguide are 1 μm wide, 220 nm in height, 50 nm in etching depth, and the radii of all five microrings are 1 mm. These parameters ensure that the fundamental mode with TE polarization could be excited at wavelength around 1550 nm and the bending loss can be ignored while the propagation loss caused by imperfect fabrication is considered as a typical value of 0.5 dB cm^{-1} [13]. The free spectral range (FSR) of such an MPF is 12 GHz, which is determined from the microring circumference of 6283.185 μm. It should be mentioned that the central frequency of MPF could be varied by appropriately designing the radius of the MR. The spacing between adjacent rings is 3141.737 μm, which satisfies the condition of all rings responses being in-phase and the gaps between the input (output) bus and all microring waveguides is 500 nm. Other parameters of MPFs are set as $P_{\mathrm{c}} = 10$ mW, $\Re = 0.5$ A W^{-1}, $V_\pi = 1$ V, $v_{\mathrm{m}} = 0.05$ V, and the optical carrier wavelength is 1550.049 nm.

With equations (2) and (3), the optical spectrum and corresponding microwave spectrum were calculated. The results are shown in figures 3(a) and (b), respectively. Figure 3(b) depicts the microwave response with uniform feedback ratios,

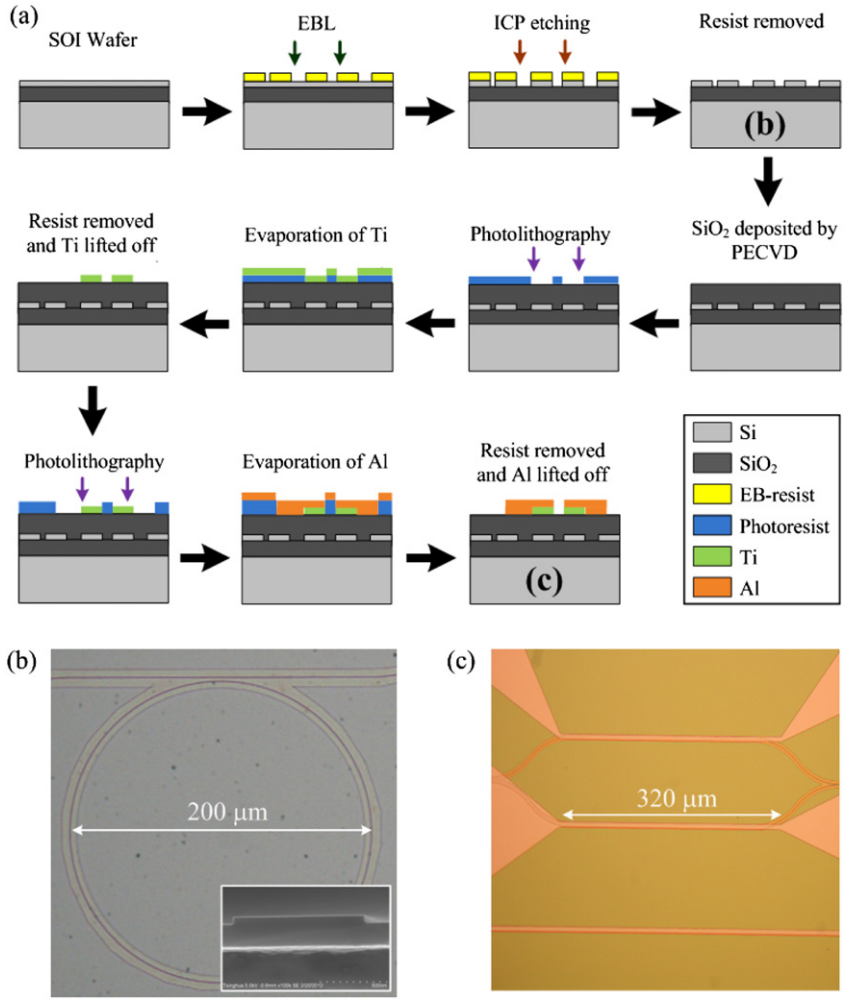

Figure 4. (a) The fabrication process of the proposed parallel-cascaded MRs assisted with an MZI. (b) Optical micrograph of the MR structure after ICP etching and the inset is a SEM image of the cross section of the waveguide. (c) Optical micrograph of MZI with heaters after the entire fabrication process.

Table 1. Summary of filter responses shown in figures figure 3(b)–(e).

A_{add}, $\Delta\phi_{\text{add}}(\times\pi)$	$\Delta\phi_{1,2}(\times\pi)$	$\text{BW}_{-3\text{ dB}}$ (GHz), SMSR (dB), SF
[1, 1, 1, 1], [2, 2, 2, 2]	[2, 2, 2, 2], [2, 2, 2, 2]	0.45, 10, 0.54
[1, 1, 1, 1], [1, 1, 1, 1]	[1, 1, 1, 1], [1, 1, 1, 1]	2.33, 21, 0.61
[0.54, 0.10, 0.81, 0.13], [2, 2, 2, 2]	[1.68, 1.53, 1.80, 1.54], [2.32, 2.47, 2.20, 2.46]	0.52, 18, 0.48
[0.80, 1.00, 0.80, 0.60], [1, 1, 1, 1]	[0.80, 1.00, 0.80, 0.70], [1.20, 1.00, 1.20, 1.30]	1.92, 24, 0.54

which means that additional complex amplitudes for each MZI is uniform as $[1e^{j2\pi}, 1e^{j2\pi}, 1e^{j2\pi}, 1e^{j2\pi}]$ (the corresponding $\Delta\phi_{1,2}$ are $[2\pi, 2\pi, 2\pi, 2\pi]$ and $[2\pi, 2\pi, 2\pi, 2\pi]$). As described above, the additional amplitude and phase can be tuned independently by proper setting of the phase shift of the two arms of the MZI. Figure 3(c) shows the response with the vector of $A_{\text{add}}e^{j\Delta\phi_{\text{add}}} = [1e^{j\pi}, 1e^{j\pi}, 1e^{j\pi}, 1e^{j\pi}]$, where only additional phase is introduced. It is clear that the bandwidth (BW) becomes wider compared to the uniform case (see figure 3(b)). So additional phase tuning can be used to obtain large-scale bandwidth adjustment, which is consistent with reported result in [10]. In spite of the bandwidth being adjusted through additional phase tuning, the sidelobes of the two former cases (see figures 3(b) and (c)) are quite high. In order to suppress the sidelobes, one method is to change the amplitude of feedback ratios by tuning the additional amplitude of the MZI output, which is similar to the apodization of grating filters. Figures 3(d) and (e) show the responses with suppression of sidelobes on the base of the two former cases respectively, and the corresponding vector of $A_{\text{add}}e^{j\Delta\phi_{\text{add}}}$ are $[0.54e^{j2\pi}, 0.01e^{j2\pi}, 0.81e^{j2\pi}, 0.13e^{j2\pi}]$ and $[0.8e^{j\pi}, 1.0e^{j\pi}, 0.8e^{j\pi}, 0.6e^{j\pi}]$. It could be found that the sidelobes are suppressed by apodization so that a box-like spectrum shape is obtained. Table 1 summaries the relevant parameters of -3 dB bandwidth ($\text{BW}_{-3\text{dB}}$), side-mode suppression ratio (SMSR), and shape factor (SF) (defined as

$BW_{-3dB}/BW_{-10\ dB}$) of the filter responses shown in figures 3(b)–(e). These results indicate that the filter response can be reconfigured to meet the requirement of flexible signal processing with our proposed structure and tuning method.

4. Fabrication method and discussion

To illustrate the feasibility of fabricating the proposed structure, the fabrication process as shown in figure 4(a) could be employed, which is similar to [14]. In our proposed structure, the basic elements are MRs and MZIs. Both of them can be fabricated on SOI wafers with a 220 nm thick top silicon layer. Firstly, a CAD-drawing must be prepared as the designed parameters. Then the drawn pattern is transferred to an SOI wafer with electron-beam lithography (EBL) and inductively coupled plasma (ICP) etching with etching depth of 60 nm. Figure 4(b) is an optical micrograph of our fabricated MR after ICP etching and the inset is a scanning electron microscope (SEM) image of a cross section of waveguide. Here the radius of MR is 0.1 mm and the width and height of the waveguide are 1 and 0.22 μm respectively. Actually, MRs with other sizes and MZIs could also be fabricated according to such a process.

After the proposed structure with MRs and MZIs on SOI is obtained, thermal or electrical tuning elements would be fabricated. Here, micro-heaters are considered as the tuning elements. Firstly, an appropriately thick SiO_2 cladding layer (typical 1–2 μm thick) is deposited by plasma-enhanced chemical-vapor deposition (PECVD) for isolating the heaters and waveguides. Then, heaters and electrical contact pads were sequentially patterned with photolithography, evaporation, and lift-off processes. The materials of titanium (Ti) and aluminum (Al) are usually chosen for heaters and electrical contact pads, respectively. Following the entire fabrication process, the proposed structure with thermal tuning elements can be prepared. An optical micrograph of an MZI with micro-heaters is shown in figure 4(c). In this work, thermal tuning is proposed due to the simpler fabrication process and wide tuning range. It has been demonstrated that the thermal tuning speed could achieve tens of kilohertz [15], which may be enough for most reconfigurable MPFs. If higher tuning speed is required, p–n junctions could be employed as the tuning element; the fabrication process can be found in [16].

5. Conclusion

In summary, we propose a new structure of reconfigurable MPFs based on MZI assisted parallel-cascaded silicon MRs. With the help of MZIs, the filter response can be reconfigured by changing the feedback ratios. The simulation results indicate that the BW of filter response could be varied from 0.45 to 2.33 GHz by controlling the phase shifter of the MZI and the SMSR can be enhanced from 10 to 18 dB by additional amplitude apodization. As the optoelectronics integration technology matures, it can be expected that MPFs based on MZI assisted parallel-cascaded silicon MRs will be realized and applied to communication systems.

Acknowledgments

This work was supported by the National Basic Research Program of China (Nos 2011CBA00608, 2011CBA00303, 2011CB301803, and 2010CB327405), the National Natural Science Foundation of China (Grant Nos 61036011 and 61036010), and the Project of Science and Technology at the Communication Information Security Control Laboratory. The authors would like to thank Drs W Zhang, F Liu, and K Y Cui for their valuable discussions and helpful comments.

References

[1] Capmany J, Ortega B and Pastor D 2006 A tutorial on microwave photonic filters *J. Ligthwave Technol.* **24** 201–29
[2] Capmany J, Pastor D and Ortega B 1999 New and flexible fiber-optic delay-line filters using chirped Bragg gratings and laser arrays *IEEE Trans. Microwave Theory Tech.* **47** 1321–6
[3] Capmany J, Mora J, Ortega B and Pastor D 2005 Microwave photonic filtersusing low-cost sources featuring tunability, reconfigurability and negative coefficients *Opt. Express* **13** 1412–7
[4] Barkai A, Chetrit Y, Cohen O, Cohen R, Elek N, Ginsburg E, Litski S, Michaeli A, Raday O and Rubin D 2007 *J. Opt. Netw.* **6** 25–47
[5] Pile B and Taylor G 2009 An investigation of the operation and performanceof coherent microwave photonic filters *IEEE Trans. Microwave Theory Tech.* **57** 487–95
[6] Rasras M, Tu K, Gill D, Chen Y, White A, Patel S, Pomerene A, Carothers D, Beattie J and Beals M 2009 Demonstration of a tunable microwave-photonic notch filter using low-loss silicon ring resonators *J. Ligthwave Technol.* **27** 2105–10
[7] Palaci J, Villanueva G E, Galan J V, Marti J and Vidal B 2010 Single bandpass photonic microwave filter based on a notch ring resonator *IEEE Photon. Technol. Lett.* **22** 1276–8
[8] Zhang D, Feng X and Huang Y 2012 Simulation of 60 GHz microwave photonicfilters based on serially coupled silicon microring resonators *Chin. Opt. Lett.* **10** 021302
[9] Little B E, Chu S T, Hryniewicz J V and Absil P P 2000 Filter synthesis forperiodically coupled microring resonators *Opt. Lett.* **25** 344–6
[10] Melloni A 2001 Synthesis of a parallel-coupled ring-resonator filler *Opt. Lett.* **26** 917–9
[11] Little B, Chu S, Haus H, Foresi J and Laine J 2002 Microring resonator channel dropping filters *J. Ligthwave Technol.* **15** 998–1005
[12] Ye T and Cai X R 2010 On power consumption of silicon-microring-based optical modulators *J. Ligthwave Technol.* **28** 1615–23
[13] Dong P *et al* 2010 GHz-bandwidth optical filters based on high-order silicon ring resonators *Opt. Express* **18** 23784–9
[14] Dong P, Qian W, Liang H, Shafiiha R, Feng N N, Feng D Z, Zheng X Z, Krishnamoorthy A V and Asghari M 2010 Low power and compact reconfigurable multiplexing devices based on silicon microring resonators *Opt. Express* **18** 9852–8
[15] Gan F, Barwicz T, Popovic M A, Dahlem M S, Holzwarth C W, Rakich P T, Smith H I, Ippen E P and Kartner F X 2007 Maximizing the thermo-optic tuning range of silicon photonic structures *Conf. Photonics in Switching (San Francisco, CA) IEEE* pp 67–8
[16] Gardes F Y, Thomson D J, Emerson N G and Reed G T 2011 40 Gb s^{-1} siliconphotonics modulator for TE and TM polarisations *Opt. Express* **19** 11804–14